

This Issue:

Special Issue on Ultraviolet

In This Issue

Articles

Higher Energy Photons Arrive at GSICS

by Larry Flynn, NOAA

In-flight Characterization of the Solar Diffuser of GOME-2 on Metop-A

by Ruediger Lang, EUMETSAT

Use of Solar Reference Spectra for Satellite Instruments

by Matthew DeLand, SSAI

The Absorbing Aerosol Index

by Omar Torres, NASA

Ozone Measurements from FY-3A

by Weihe Wang, CMA

Measurement of Atmospheric Composition using UV-visible Spectrometers from Geostationary Orbits

by Jhoon Kim, Department of Atmospheric Sciences, Yonsei University, Seoul, Korea

The MAESTRO Spectrophotometer on the Atmospheric Chemistry Experiment

by C.T. McElroy, York University, Canada

News in This Quarter

The NASA Orbiting Carbon Observatory-2 is on its Way!

by David Crisp, NASA

GRUAN-GSICS-GNS SRO WIGOS Workshop on Upper-Air Observing System Integration and Application

by Tim Hewison, Xavier Calbet, and Axel von Engel, EUMETSAT

Summary of GSICS Executive Panel Meeting

by Jerome Lafeuille, WMO

A Note from the Executive Panel Chair

by Peng Zhang, CMA

Announcements

GSICS Users Workshop to be Held

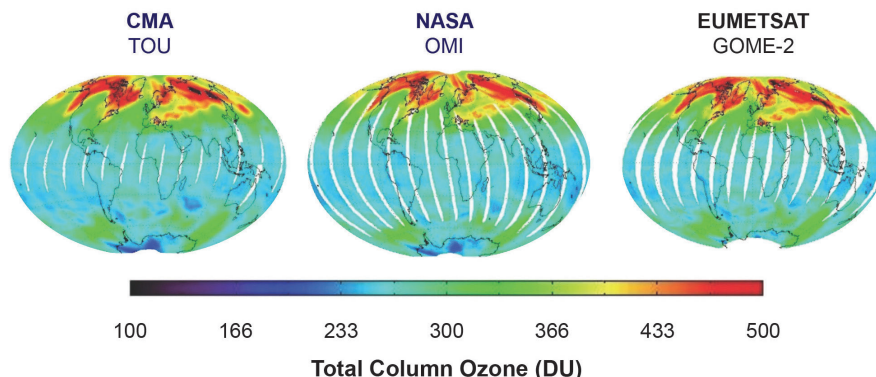
19-21 Nov, 2014 in Shanghai

by Manik Bali, NOAA

GSICS Lunar Calibration Workshop to be Held in Darmstadt, Germany

by Sebastien Wagner, EUMETSAT, T. Stone, USGS, S. Lachérade, CNES, B. Fougner, CNES, and X. Xiong, NASA

GSICS-Related Publications



Global total column ozone distribution of March 21, 2009 observed by CMA (FY-3A), NASA (OMI) and EUMETSAT (GOME-2)

Higher Energy Photons Arrive at GSICS

by Larry Flynn, NOAA

This issue of *GSICS Quarterly* features a new area of the spectrum for GSICS work, the *ultraviolet*. Unlike some other spectral regions, the primary products for the *backscatter ultraviolet* (BUV) measurements are the ratios of earth radiances to solar irradiances. These ratios provide information on atmospheric absorption and scattering, and on cloud and surface reflectivity for product retrieval algorithms.

The use of ratios has inherent cancellation of some instrument throughput changes, although the resources and philosophies to track the varying instrument components differ among the instruments. For example, the Ozone Mapping Profiler Suite (OMPS) instruments use pairs of working and reference diffusers to monitor the diffuser changes and identify the changes in the rest of the optical and sensor characteristics over time with a parameter called Calibration Factor Earth, CFE(t). A simplistic representation of the adjusted ratios (related to top-of-atmosphere reflectance) has the form

$$[\text{Earth_radiance}(t) * 1/\text{CFE}(t)] / [\text{Day1_Solar_irradiance} * \text{AD}(t)]$$

where AD(t) adjusts for the changes in the Earth/Sun distance, while the GOME-2 series of instruments use onboard sources to monitor the solar diffuser changes over time, SDC(t), independent of the rest of the optical and sensor changes, and make daily solar measurements. The simplistic representation of the adjusted ratios has the form

$$\text{Earth_radiance}(t) / [\text{Solar_irradiance}(t) * 1/\text{SDC}(t)]$$

Product retrieval algorithms for BUV measurements are further designed to be insensitive to other calibration uncertainties or to identify them internally. See, for example, Herman et al. (1991) and Platt et al. (1979), and later works citing them.

The Ultraviolet Subgroup of the GSICS Research Working Group has been coming together over the last year. Rose Munro has agreed to chair the subgroup. The subgroup has four initial projects, three of which are represented in papers in this quarterly. The fourth is discussed briefly in this overview article. All of the projects are initially working with BUV measurements from instruments on polar-orbiting platforms.

GSICS members are asked to designate participants for the UV subgroup and identify contacts for each of the four projects. Information can be sent to the chair, Rosemary.Munro@eumetsat.int. The four initial projects and the three related papers are as follows:

1. Best practices for BUV on-ground and in-flight calibration and characterization. This project seeks to build on the lessons learned from past instruments to identify the key areas of calibration that will most benefit the mission goals. It is also recognized that sharing calibration assets across missions is efficient and beneficial. Examples of the roles of in-orbit and pre-flight calibration for the GOME-2 instruments are provided in the article by Ruediger Lang, “In-flight Characterization of the Solar Diffuser of GOME-2 on Metop-A.”

2. Solar UV measurement project. This project’s goal is to create quantitative comparisons among the solar spectra measured by the different instruments. Some of the issues in this work are identified in the article by Matthew DeLand, “Use of Solar Reference Spectra for Satellite Instruments,” discussing limits and considerations for solar spectra.

3. Calibration of reflectivity and aerosol channels. This project’s goals are to develop vicarious calibration

methods and provide comparisons for monitoring the BUV measurements for channels with little trace gas absorption, primarily from 340 nm to 405 nm. The article by Omar Torres, “The Absorbing Aerosol Index,” is a primer on the UV Absorbing Aerosol Index products. Notice that the statement within it—“For a well calibrated sensor the AAI is close to zero in the absence of aerosols and clouds”—can be inverted to give a check on inter-channel calibration for regions with known clear sky and low aerosol loading. Approaches for checking reflectivity channel calibration will follow the work in Jaross and Krueger (1993), where they looked at using ice radiances to characterize time-dependent changes in reflectivity channel performance. Additional target regions have been identified and used by BUV practitioners since then.

4. Calibration comparisons for 240 nm to 300 nm. The fourth project seeks to develop comparisons of radiance/irradiance ratios from 240 nm to 300 nm. The basic idea is to use a model atmosphere (from climatology, assimilation, or other sources) with a radiative transfer (RT) forward model to predict the radiance/irradiance ratios for two instruments viewing the same region. The results of the RT model results are used as a transfer to compare the measurements.

This method is currently applied to the NOAA POES SBUV/2 instrument by creating measurement residuals by using the Version 8 SBUV/2 profile retrieval algorithm (see Figure 1, V8Pro) first guess and forward model to generate the RT results.

The Version 8 algorithm a priori ozone profiles and forward model have been used to allow direct comparison of the radiance/irradiance ratios for the two instruments. NOAA-16 was an afternoon satellite and NOAA-17 was a morning satellite during this period. By the end of the record, the NOAA-16 satellite was in a late-afternoon orbit. Similar comparisons have been used to create a homogenous record from the SBUV/2

instruments series (DeLand et al., 2012). Related methods have been used to track the calibration of individual instruments. See, for examples, Bhartia et al. (1995) and van der A et al. (2002). The first article also addresses the interaction of solar zenith angles and the wavelength dependence of ozone cross-sections.

In addition to these, we have articles on the following:

1. The TOU instruments on CMA FY-3 series of satellites. The article by Weihe Wang, “Ozone Measurements from FY-3A,” presents a successful application of a method for vicarious cross-sensor calibration demonstrated for the TOU on FY-3A by using EOS Aura OMI ozone estimates to specify the atmosphere for a RT forward model.

2. The GEMS, TEMPO and Sentinel-4 missions. The article by Jhoon Kim, “Measurement of Atmospheric Composition using UV-visible Spectrometers from Geostationary Orbits,” describes these planned missions/instruments which will add geostationary assets to the BUV satellite complement. We look forward to the use of LEO/GEO comparison techniques as measurements from these new instruments become available.

Even before they become available there will be a new BUV/Visible instrument, EPIC (Information on EPIC is available at directory.eoportal.org/web/eoportal/satellite-missions/d/dscovr), operating from L1 and opening new areas for LEO/L1 and GEO/L1 underflight comparisons. Looking back in time, the BUV experience on underflights already includes SS/LEO (Space Shuttle underflights of LEO) comparisons. (A bibliography of papers on SSBUV underflights of the SBUV/(2) instruments can be found at disc.sci.gsfc.nasa.gov/ozone/documentation/publications/sensor/ssbuv_pubs.shtml).

3. The MAESTRO Spectrophotometer on the CSA SCISAT satellite. The article by C.T. McElroy, “The MAESTRO Spectrophotometer on the Atmospheric Chemistry Experiment,” gives an introduction to the instrument designs

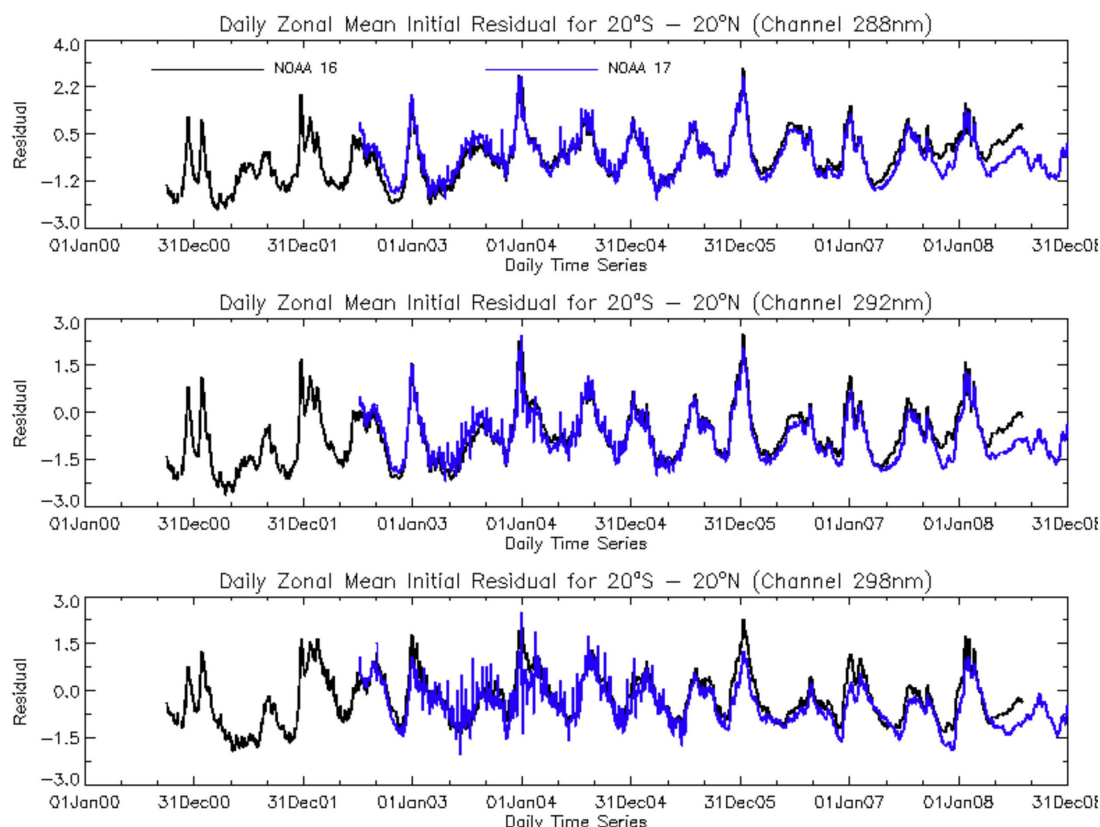


Figure 1. These three plots show the initial measurement residuals (daily zonal means for 20S to 20N) for three profile wavelengths (Top 288 nm, Middle 292 nm, and Bottom 298 nm) for the V8Pro product for the equatorial daily zonal means (20N to 20S). The two sets of data are for the NOAA-16 SBUV/2 and the NOAA-17 SBUV/2. The residual units are N-values (~2.3%).

and products of ACE. The MAESTRO instrument has been providing a high-quality set of atmospheric composition variables from solar occultation measurements for the last ten years.

References

- Bhartia, P. K., Taylor, S., McPeters, R.D., and Wellemeyer, C., 1995, Application of the Langley plot method to the calibration of the solar backscattered ultraviolet instrument on the Nimbus 7 satellite, *J. Geophys. Res.*, 100(D2), 2997–3004, doi: 10.1029/94JD03072.
- DeLand, M.T., Taylor, S.L., Huang, L.K., and Fisher, B.L., 2012, Calibration of the SBUV version 8.6 ozone data product. *Atmos. Meas. Tech.*, 5, 2951–2967, doi:10.5194/amt-5-2951-2012.
- Herman, J. R., Hudson, R., McPeters, R., Stolarski, R., Ahmad, Z., Gu, X.Y., Taylor, S., and Wellemeyer, C., 1991, A new self-calibration method applied to TOMS and SBUV backscattered ultraviolet data to determine long-term global ozone changes. *J. Geophys. Res.*, 96, 7531–7545.
- Jaross, G. and Krueger, A. J., 1993. Ice radiance method for UV instrument monitoring. *Proc. SPIE Int. Soc. Opt. Eng.*, 2047, 94–101.
- Platt, U., Perner, D., and Pätz, H.W., 1979, Simultaneous measurement of atmospheric CH₂O, O₃, and NO₂ by differential optical absorption. *J. Geophys. Res.*, 84, 6329–6335.
- Van der A, R. J., van Oss, R.F., Pitters, A.J.M., Fortuin, J.P.F., Meijer, Y.J., and Kelder, H.M., 2002, Ozone profile retrieval from recalibrated Global Ozone Monitoring Experiment data, *J. Geophys. Res.*, 107(D15), doi: 10.1029/2001JD000696.

[Rate and comment on this article](#)

In-flight Characterization of the Solar Diffuser of GOME-2 on Metop-A

by Ruediger Lang, EUMETSAT

Instruments in space measuring the solar irradiance—either for monitoring the solar activity directly or for use as a reference in order to derive the Earth albedo—must introduce measures to reduce absolute radiance levels of incoming light. This is a key design element in order to avoid a saturation of detectors and to mitigate the effect of potentially damaging contamination-inducing radiation on other optical elements along the light path (Slijkhuis et al. 2004).

The optical design of GOME-2 is such that both radiance and irradiance measurements share a common optical path up to the detector, with the diffuser being the only additional optical element not shared between them. Details of the design and the measurements of GOME-2 are provided in EUM/OPS/DOC/10/1299 and EUM/OPS-EPS/REP/09/0619, Version 1F.

Mischaracterization of the diffuser bidirectional scattering distribution function (BSDF) on-ground and changes in the diffuser characteristics between on-ground and in-flight, as well as in-flight diffuser degradation, will lead to a reduced quality of the measured reflectance. Mischaracterization of the BSDF in elevation direction (the Sun passing through the slit at a fixed azimuth angle during one solar measurement sequence, usually on the order of a couple of minutes) can lead to a bias introduced on the averaged solar mean reference (SMR) spectrum at any given wavelength. Mischaracterization of the BSDF in azimuthal direction and spectral domain leads to seasonal biases and interferences with spectral absorption patterns, respectively. The latter introduces biases in trace gas column and profile retrievals (Slijkhuis et al. 2004 and reference therein).

Here we present the analysis of in-flight derived BSDF from daily GOME-

2/Metop-A measurements, in orbit since October 2006. For this instrument we analyzed all solar azimuth angles for a reference period of 1 year (August 2011 through July 2012). In this late period of the mission, the instrument degradation at all wavelengths, which has to be accounted for in the analysis, is significantly more stable, while during the early years not only was the degradation rate much stronger but also mission outages were much more frequent (EUM/OPS/DOC/10/1299).

Figure 1 shows the fully calibrated level-1b irradiance signal at 330 nm normalized to 1 August 2011, which makes use of the BSDF as measured on-ground. The wiggles around February and June 2012 indicate some non-perfect azimuthal characterization of the BSDF.

Looking over the whole mission period, they are found to reappear on a seasonal basis.

In this figure, the signal without the radiometric and BSDF response, but including all other calibration steps, is shown as the blue line. This signal shows that the azimuthal variations (wiggles) are a real feature of the diffuser but are not perfectly taken out with the on-ground BSDF calibration parameters.

The green line shows the level-1A signal without the radiometric and BSDF response and corrected for the degradation at 330 nm during this 1-year period (red line) based on the latest version of the GOME-2/Metop-A degradation model version 0.9. The degradation-corrected signal (corresponding to the

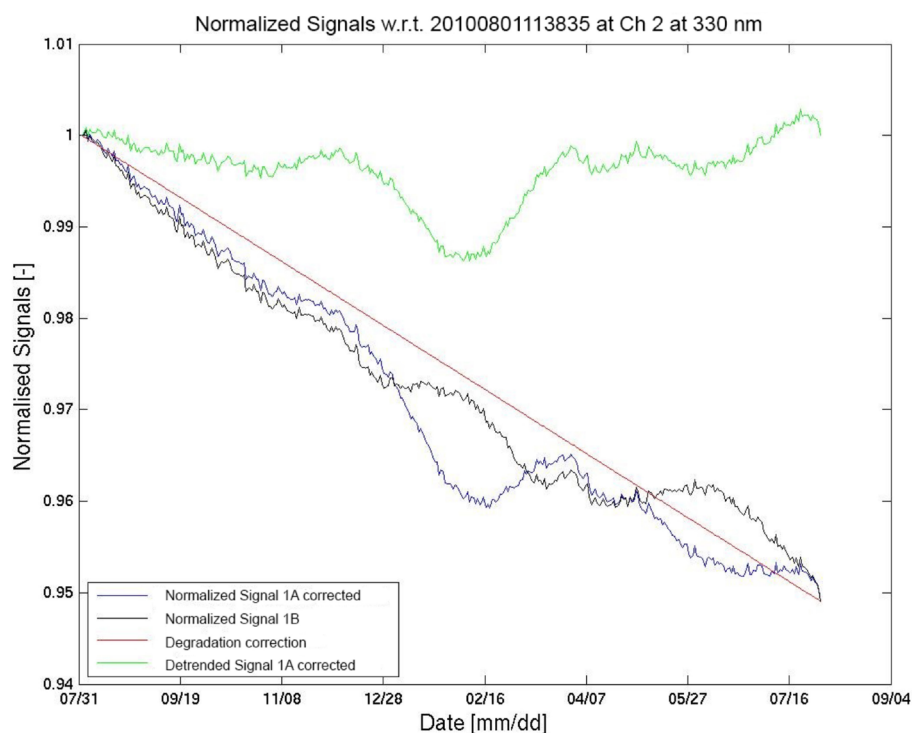


Figure 1. Fully calibrated GOME-2/Metop-A level 1B normalized irradiance signal (black line) at 330 nm during the period of August 2011 to July 2012. For details see body of the text.

green line as shown for 330 nm) at each of the 4096 wavelengths between 240 and 800 nm for the main channels and for the 256 wavelength measurements of the two polarization measurements devices (PMDs) will now be used in the further analysis.

To evaluate the final in-flight derived BSDF, measurements over all elevation angles ($\pm 1.5^\circ$ around the center of the slit) and from all solar azimuth positions acquired over the year (between 317° and 333°) are sorted and then normalized with respect to the geometric center at elevation angle 0° and azimuth angle 325° . In order to arrive at the final irradiance, i.e., the Mueller matrix element (MME_{irr}) to carry out the radiometric calibration of the irradiance signal, the BSDF is finally multiplied by the on-ground characterized irradiometric response function of each channel.

Figure 2 shows in-flight derived and on-ground characterized MMEs of the irradiance radiometric calibration at 330 nm, showing different dependencies in both elevation and azimuth direction. The on-ground data have much lower resolution in both elevation angle (0.75° for on-ground and 0.1° for in-flight data) and azimuth dimension (2.0° for on-ground and 0.5° for in-flight data). The low resolution in elevation angle cannot capture the observed sinusoidal dependence, which is introduced by shadowing effects of a mesh which is located in front of the diffuser in order to reduce the potential amount of spectral interferences. Different azimuthal behaviour is also observed, especially for highest and lowest azimuth angles. These differences are responsible for the reoccurring wiggles seen over the year at many wavelengths in the solar irradiance data time series.

Finally, Figure 3 shows the difference between a SMR derived for 16 December 2007 by applying the on-ground MME and an SMR using the in-flight derived MME at all main channel wavelength. The residual between both SMRs shows small-scale spectral structures and some etalon-like variations at longer periods. The latter are very likely intro-

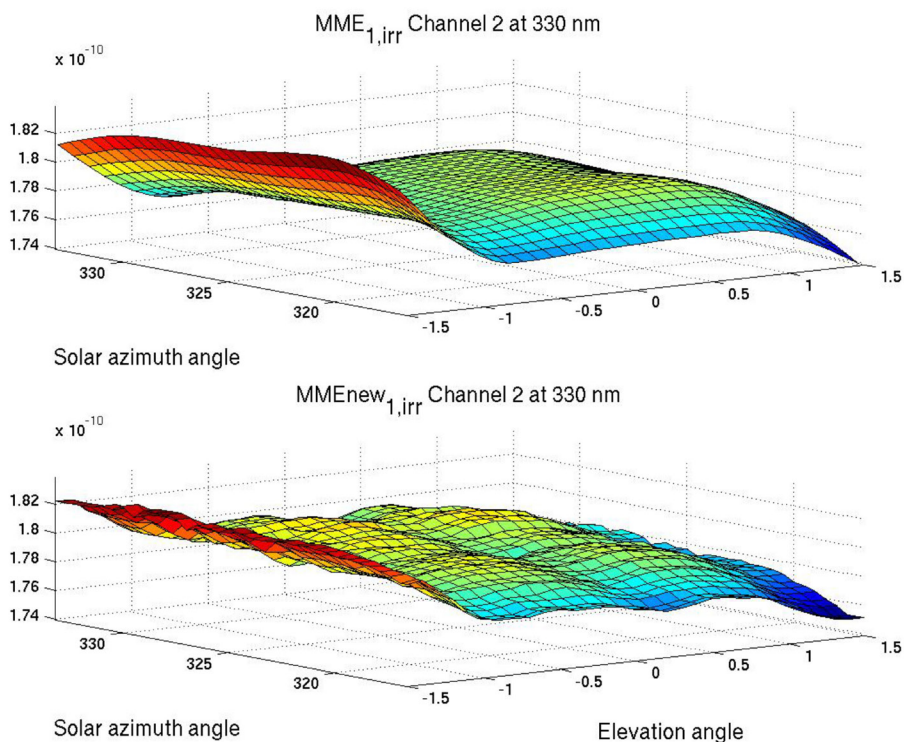


Figure 2. Comparison of pre-flight (top) and in-flight (bottom) Mueller matrix elements (MMEs) at 330 nm for the radiometric calibration of the irradiance signals.

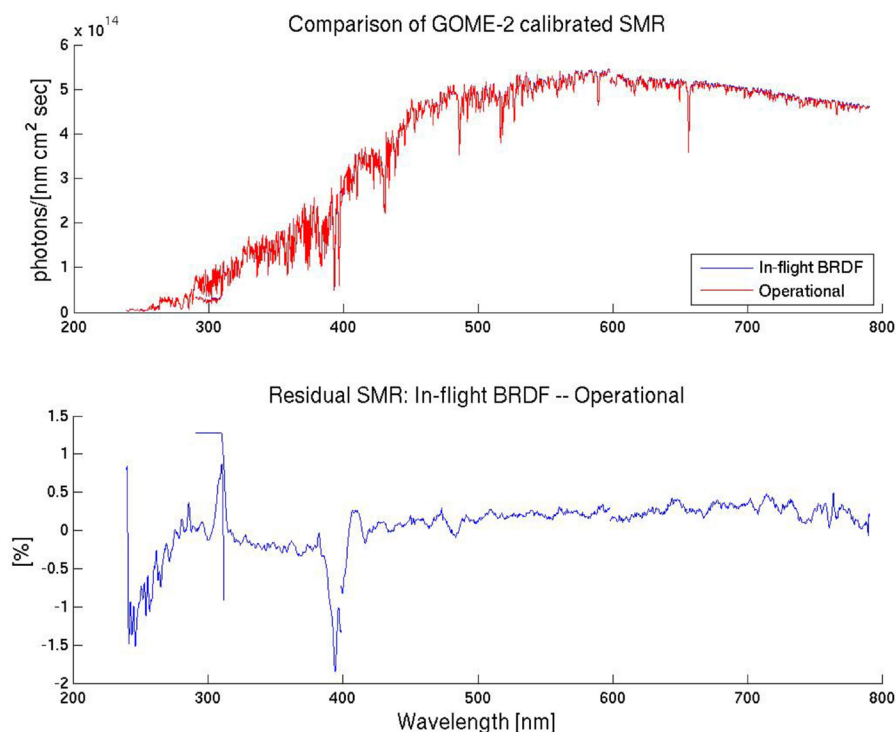


Figure 3. Solar Mean reference spectrum (top panel) and residual (lower panel) acquired using the on-ground and the in-flight derived BSDF diffuser characterization. In the top panel, the in-flight results are below the operational version red line results.

duced during the on-ground characterization, since under ambient conditions it is very difficult to perfectly thermally stabilize and remove (through normalization) the etalon introduced by water layers at the detector level.

References

Slijkhuis, S., Wahl, S., Aberle, B., and Loyola, D., 2004, Re-analysis of GOME/ERS-2 diffuser properties, *Envisat & SRS Symposium*, Salzburg, Austria.

[GOME-2 Factsheet, EUM/OPS/DOC/10/1299, Version 4A](#)

[GOME-2/Metop-A Level 1B Product Validation Report No. 5, Version 1F](#)

[Rate and comment on this article](#)

Use of Solar Reference Spectra for Satellite Instruments

by Matthew DeLand, SSAI

The extraterrestrial solar irradiance (i.e., measured outside Earth's atmosphere) has numerous benefits as a calibration source for remote sensing satellite instruments. For example:

- It is available for an extended period of time during every orbit.
- Its intensity is high across a wide spectral range.
- It is, for much of the spectrum, extremely stable compared to any onboard calibration source. And, in regions where it is not stable, the variations are often highly correlated.
- Many spectral features are available for use in wavelength calibration.

Each of these benefits also brings some challenge in terms of instrument design and data analysis:

- The constant presence of solar illumination requires instrument designers to limit exposure of optical surfaces to minimize degradation, particularly at UV wavelengths.
- Solar irradiance can be stronger than terrestrial radiance at a given wavelength by factors ranging from 10^2 to 10^4 , which must be considered when designing the optical system and instrument electronics.
- Solar irradiance does have natural variability at UV wavelengths (particularly below 300 nm), with time scales ranging from minutes to years.
- The solar spectrum incorporates millions of emission and absorption features, so that the exact irradiance

spectrum produced by any instrument will depend on its characteristics and design.

In order to use the Sun as a calibration source, it is necessary to first have a reference spectrum to understand what the instrument is expected to see. This article will briefly describe some published reference solar spectra, and issues that users should be aware of when selecting a dataset for their own use.

Overview

It is important for users to realize that no single instrument measures solar irradiance at high resolution simultaneously over all spectral regions of interest (X-ray, UV, visible, IR). Thus, any reference solar spectrum is typically a composite of measurements from multiple instruments, taken at different times, and often with varying spectral resolution. In addition, the final reference spectrum may incorporate radiometric adjustments based on comparisons with lower resolution measurements. Differences in spectral resolution and sampling are particularly important in the UV, where many deep Fraunhofer lines occur. The next section presents basic information about some reference solar spectra published during the last decade. Table 1 summarizes specific parameters for each spectrum.

Reference Solar Spectra

ATLAS. The solar reference spec-

tra created by Thuillier et al. (2004) take advantage of the ATLAS missions conducted in the early 1990s, when three solar irradiance instruments (along with other remote sensing instruments) were flown together on the NASA Space Shuttle. The UARS satellite (carrying two additional solar instruments) was also operating during this period, so that up to five datasets were available for some spectral regions. Thuillier et al. selected reference dates during the ATLAS-1 and ATLAS-3 missions (29 March 1992 and 11 November 1994, respectively) to construct spectra corresponding to moderately high and moderately low levels of solar activity. Each spectrum covers the spectral range 0.5-2,400 nm, using rocket data for the EUV region below 120 nm. They created average irradiance values for UV spectral regions where multiple data sets were present. They also used the high resolution model spectrum of Kurucz (1995) to insert spectral features into lower-resolution measurements in the visible and IR regions.

KNMI. Dobber et al. (2008) created a high resolution solar reference spectrum covering 250–550 nm to support on-orbit calibration of the OMI instrument on the EOS Aura satellite. Very high resolution data from AFGL balloon measurements (Hall and Anderson, 1991) and KPNO ground-based measurements (Kurucz et al., 1984) were convolved to a slightly lower resolution, and then adjusted radiometrically through

Table 1. Summary of Solar Reference Spectra

Name WvL Sampling	Sources	Resolution	Time	Calibration	Accuracy
ATLAS 0.5–2400 nm 0.5–120 nm: 1 nm 120–400 nm: 0.05 nm 400–2400 nm: 0.2–0.6 nm	0.5–120 nm: Rocket 120–200 nm: UARS SOLSTICE, UARS SUSIM 200–400 nm: UARS SOLSTICE, UARS SUSIM, ATLAS SUSIM, SSBUV, SOLSPEC 400–870 nm: SOLSPEC 870–2400 nm: SOSP	0.5–120 nm: 1.0 nm 120–400 nm: 0.25 nm (smoothed) 400–2,400 nm: 0.5 nm (degraded model)	0.5–120 nm: 1991 rocket 120–2400 nm: 29 Mar 1992 for ATLAS-1, 11 Nov 1994 for ATLAS-3	Satellite data + normalization of integrated TSI	0.5–120 nm: 30–40% 120–2,400 nm: 2–4%
KNMI 250–550 nm 0.01 nm	200–310 nm: AFGL balloon 300–550 nm: KPNO	0.025 nm (convolved)	Multiple dates	Adjusted based on comparison with low resolution data (UARS SUSIM)	< 5% for 300–550 nm
WHI 0.1–2400 nm 0.01 nm	0.1–6 nm: TIMED XPS 6–106 nm: MEGS EVE (rocket) 106–116 nm: TIMED SEE 116–310 nm: SORCE SOLSTICE 310–2400 nm: SORCE SIM	0.1–310 nm: 0.1 nm 310–2400 nm: 1–30 nm	Quiet: 10–16 Apr 2008 Active: 25–29 Mar 2008, 29 Mar – 4 Apr 2008	Satellite data + normalization of integrated TSI to SORCE TIM	0.1–116 nm: 10–15% 116–2,400 nm: 2–4%
SAO 2010 200–1000 nm 0.01 nm	200–300 nm: AFGL 300–1,000 nm: KPNO	0.04 nm (convolved)	Multiple dates	Adjusted based on comparison with low resolution data (ATLAS-1)	< 5% for 300–1,000 nm

comparisons with UARS SUSIM data (Floyd et al., 2003) and balloon data (Gurlit et al., 2005). It should be noted that any terrestrial measurements of absolute solar irradiance must also account for absorption effects due to the Earth's atmosphere.

WHI. During the most recent solar minimum between Cycles 23 and 24, a focused program called the Whole Heliosphere Interval (WHI) collected approximately simultaneous solar measurements at minimum activity conditions from X-ray to IR wavelengths. Woods et al. (2009) used rocket measurements to supplement operational satellite measurements over a wide spectral range (0.1–2,400 nm) and produce three reference spectra representing active and quiet conditions during March–April 2008. The primary data sources are EVE rocket data in the X-ray and EUV regions, SORCE SOLSTICE data in the FUV and MUV, and SORCE SIM data from the NUV to the IR. The

only radiometric adjustment came from comparison of the integrated reference spectrum to SORCE TIM total solar irradiance data.

SAO 2010. Chance and Kurucz (2010) have also produced a solar reference spectrum using the AFGL balloon data and the KPNO ground-based data, in this case covering the spectral range 200–1000 nm. They used a revised analysis of the KPNO data, and normalized those data to the Thuillier et al. (2004) ATLAS-1 spectrum longward of 300 nm.

Effects of Resolution and Sampling

Differences in spectral resolution, either from the original measurements or from later re-convolution, and in dataset sampling should be considered when selecting a solar reference spectrum. To illustrate this point, Figure 1 shows irradiance data between 300–320 nm from each of the reference spectra described here. While the KNMI and SAO 2010

spectra are both based on KPNO data and sampled at 0.01 nm, the slightly broader bandpass used for SAO 2010 is evident in Figure 1(b). The WHI spectrum shown in Figure 1(d) is reported at 0.1 nm sampling over its entire range, but the change in resolution between SOLSTICE and SIM data at 310 nm is clear.

Conclusion

Numerous solar irradiance reference spectra, created by combining multiple data sets, are currently available. These spectra can differ in spectral resolution and sampling by a factor of 10. The quoted accuracy of each spectrum is typically 2–4% at UV and visible wavelengths, but differences between spectra can show larger variations locally. Choosing a specific reference spectrum for regular use should be guided by user requirements.

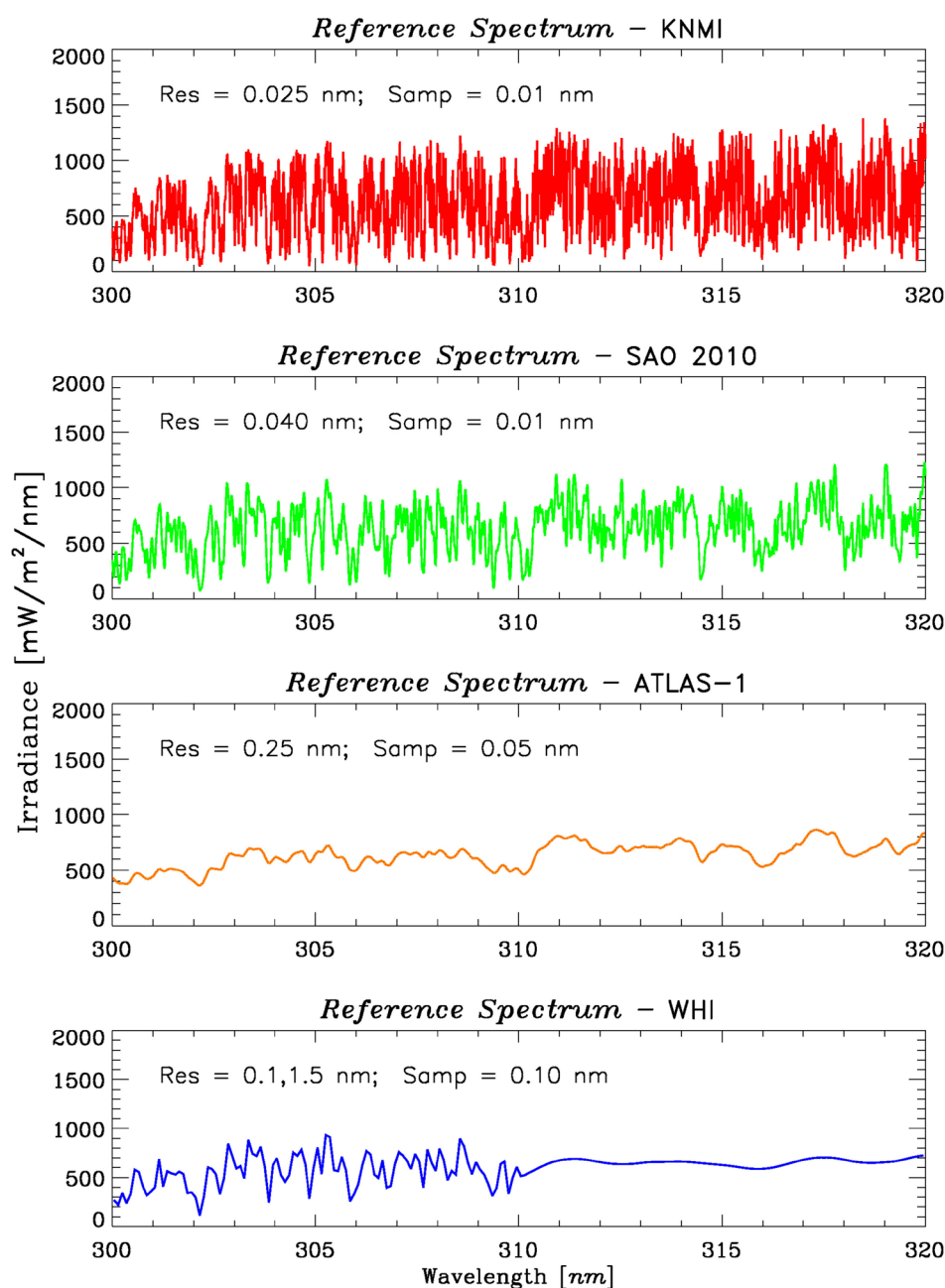


Figure 1. Sample data at 300–320 nm from different solar reference spectra. (a) = KNMI, (b) = SAO 2010, (c) = ATLAS-1, (d) = WHI. Res = resolution, Samp = sampling.

References

Chance, K., and Kurucz, R. L., 2010, An improved high resolution solar reference spectrum for earth's atmosphere measurements in the ultraviolet, visible, and near infrared. *J. Quant. Spect. Rad. Trans.*, 111, 1289–1295.

Dobber, M., Voors, R., Dirksen, R., Kleipool, Q., and Levelt, P., 2008, The high resolution solar reference spectrum between 250 and 550 nm and its application to measurements with the Ozone Monitoring Instrument. *Solar Phys.*, 249, 281–291.

Floyd, L., Rottman, G., DeLand, M., and Pap, J., 2003, Eleven years of solar UV irradiance measurements from UARS. *Proc. ISCS 2003 Symposium "Solar Variability as an Input to the Earth's Environment, SP-535*, ESA, Noordwijk, p. 195–203.

Gurlit, W., Bösch, H., Bovensmann, H., Burrows, J.P., Butz, A., Camy-Peyret, C., Dorf, M., Gerilowski, K., Lindner, A., Noël, S., Platt, U., Weidner, F., and Pfeilsticker, K., 2005, The UV-A and visible solar irradiance spectrum: inter-comparison of absolutely calibrated, spectrally medium resolution solar irradiance spectra from balloon- and satellite-borne measurements. *Atmos. Chem. Phys.*, 5, 1879–1890.

Hall, L. A., and Anderson, G.P., 1991, High resolution solar spectrum between 2000 and 3100 Å. *J. Geophys. Res.*, 96, 12,927–12,931.

Kurucz, R.L., 1995, in *Proc. 17th Annual Conference Transmission Models* (ed. G. P. Anderson), p. 333.

Kurucz, R. L., Furenhild, I., Brault, J., and Testermann, L., 1984, Solar flux atlas from 296 to 1300 nm, *National Solar Observatory Atlas No. 1*, Sunspot, NM.

Thuillier, G., Floyd, L., Woods, T.N., Cebula, R., Hilsenrath, E. Hersé, M., and Labs, D., 2004, Solar irradiance reference spectra, in *Solar Variability and its Effects on Climate, AGU Monograph 141* (ed. J. Pap), p. 171–193.

Woods, T. N., Chamberlin, P.C., Harder, J.W., Hock, R.A., Snow, M., Eparvier, F.G., Fontenla, J., McClintock, W.E., and Richard, E.C., 2009, Solar Irradiance Reference Spectra (SIRS) for the 2008 Whole Heliosphere Interval (WHI), *Geophys. Res. Lett.*, 36, L01101, doi:10.1029/2008GL036373.

[Rate and comment on this article](#)

The Absorbing Aerosol Index

by Omar Torres, NASA

The Absorbing Aerosol Index (AAI) was the fortunate unintended result of a refinement to the algorithm that since 1978 has been used for the retrieval of atmospheric total column ozone amount using measurements of backscattered ultraviolet (BUV) radiation by the Total Ozone Mapping Spectrometer sensor (Herman et al. 1997; Torres et al., 1998). The AAI is currently available on a daily basis from observations by the Aura Ozone Monitoring Instrument (OMI) and the Ozone Mapping and Profiler Suite (OMPS) on the S-NPP satellite.

The AAI is a residual quantity resulting from the difference between measured and calculated radiances (L_{λ}^* and L_{λ}^{cal} respectively) in the range 330–400 nm. The calculated radiances are obtained using a simple model of the earth-atmosphere system consisting of a molecular atmosphere bounded at the bottom by a wavelength independent Lambert Equivalent Reflector.

In the AAI algorithm the measured radiance at the top of the atmosphere is assumed to result from the combined effect of radiances originating from two pressure levels in the atmosphere representing surface, L^S , and clouds, L^C .

The L^S term is calculated for the pressure level associated with the surface while the L^C component is determined using radiative transfer calculations for an atmospheric column bounded at the bottom by a cloud layer with a cloud top at pressure P_c .

The AAI is defined as the natural logarithm of the ratio of the actually radiance L_{λ}^* to the calculated value L_{λ}^{cal} ,

$$AAI = -100 \log \left[\frac{L_{\lambda}^*}{L_{\lambda}^{cal}} \right]$$

Figure 1 shows an overlay of the OMPS AAI on the MODIS RGB for April 29, 2012 over East Asia. The presence of desert dust above clouds and over the oceans is clearly observed.

Properties

For a well calibrated sensor the AAI is close to zero in the absence of aerosols and clouds. The AAI varies between about -2.0 and 10 (or occasionally larger).

The AAI is generally positive for absorbing aerosols. Non-absorbing aerosols yield negative AI values and their magnitude depends mainly on optical depth and to a lesser extent on particle size distribution.

The AAI detects absorbing aerosols over water and all terrestrial surfaces including deserts and ice/snow covered surfaces (Hsu et al, 1999) as well as above cloud decks (Torres et al., 2012). Since water clouds yield AAI values close to zero, the AAI allows the detection of absorbing aerosols even when intermingled with clouds.

The magnitude of the AAI associated with absorbing aerosols depends on optical depth, particle size distribution,

single scattering albedo, and height of the aerosol layer above surface (Herman et al., 1997; Torres et al., 1998).

Applications

In addition to the seasonal aerosol activity associated with the annual cycles of biomass burning and desert dust mobilization across the oceans, the AAI captured extraordinary synoptic scale aerosol events of natural or anthropogenic origin that took place prior to the development of this remote sensing technique, such as the 1987 Great China Fire, the 1988 Yellowstone Fires, and the 1991 Gulf war oil fields fires (Torres and Remer, 2013).

The understanding of desert dust emission and mobilization processes has significantly advanced with the availability of the AAI product. The global distribution and frequency of occurrence of desert dust and carbonaceous aerosols was analyzed by Herman et al. (1997).

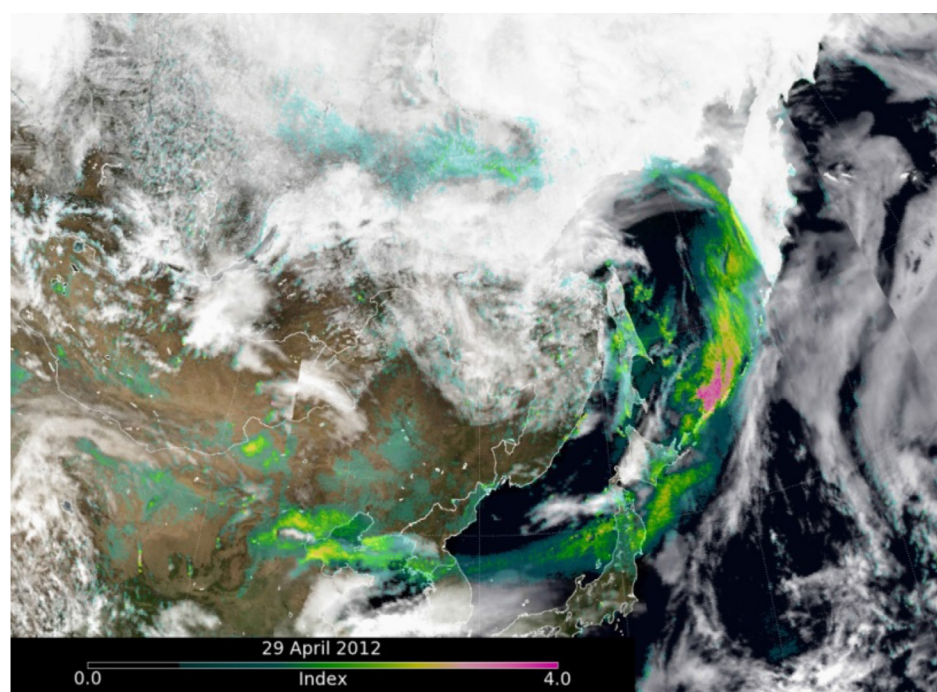


Figure 1. OMPS Aerosol Index

One of the most important contributions of the multi-year AAI record has been the identification of active desert dust sources (Prospero et al., 2002). The availability of the long-term AAI record made possible the confirmation that biomass burning aerosols frequently reach the lower stratosphere at mid and high latitudes when injected by pyro-cumulonimbus clouds formed in the aftermath of intense boreal forest fires (Fromm et al., 2008).

References

Fromm, M., Torres, O., Diner, D., Lindsey, D., Vant Hull, B., Servranckx, R., Shettle, E.P., and Li, Z., 2008, Stratospheric impact of the Chisholm pyro-cumulonimbus eruption: 1. Earth-viewing satellite perspective. *J. Geophys. Res.*, 113, doi:10.1029/2007JD009153.

Herman, J.R., Bhartia, P.K., Torres, O., Hsu, C., Seftor, C., and Celarier, E., 1997, Global distribution of UV-absorbing aerosols from Nimbus 7/TOMS data. *J. Geophys. Res.*, 102(D14), 16,911–16,922, doi:10.1029/96JD03680.

Hsu, N.C., Herman, J.R., Gleason, J.F., Torres, O., and Seftor, C.J., 1999, Satellite detection of smoke aerosols over a snow/ice surface by TOMS. *Geophys. Res. Lett.*, 26, 11651168.

Prospero, J. M., Ginoux, P., Torres, O., Nicholson, S.E., and Gill, T.C., 2002, Environmental characterization of global sources of atmospheric soil dust identified with the NIMBUS 7 Total Ozone Mapping Spectrometer (TOMS) absorbing aerosol product. *Rev. Geophys.*, 40(1), 1002, doi:10.1029/2000RG000095.

Torres O., Bhartia, P.K., Herman, J.R., Ahmad, Z., and Gleason, J., 1998, Derivation of aerosol properties from satellite measurements of backscattered ultraviolet radiation: theoretical basis. *J. Geophys. Res.*, 103, 17099–17110.

Torres, O., Jethva, H., and Barthia, P.K., 2012, Retrieval of aerosol optical depth above clouds from OMI observations: sensitivity analysis and case studies. *Journal. Atm. Sci.*, 69, 1037–1053, doi:10.1175/JAS-D-11-0130.1.

Torres, O., and Remer, L., 2013, History of passive remote sensing of aerosol from space. Ch.7 in *Aerosol Remote Sensing*, Lenoble, J., Remer, L., and Tanre, D., editors, Springer-Praxis, ISBN 978-3-642-17724-8, doi:10.1007/978-3-642-17725-5.

[Rate and comment on this article](#)

Ozone Measurements from FY-3A

by Weihe Wang, CMA

A cross-sensor calibration technique has been developed and applied to improve upon the pre-launch radiance calibration and characterization for the Total Ozone Unit (TOU) on board the FengYun-3/A (FY-3A) satellite.

The first measurements by TOU showed a large difference in solar irradiance compared with results from the Solar Backscatter Ultraviolet Radiometer (SBUV/2) on NOAA-16. The solar irradiances at channel 5 and channel 6 (see Table 1 for the spectral properties of TOU) were approximately 17 percent and 20 percent higher than the measurements made by the SBUV/2, while the other four channels (at 308 nm, 313 nm, 318 nm and 322 nm) had good agreement. Retrievals of total column ozone from TOU using the solar irradiance from the SBUV/2 showed a large difference when compared with Level 3 ozone products for the Ozone Monitoring

Table 1. Spectral Properties of TOU

Channel	Central Wavelength (nm)	FWHM (nm)
1	308.727	1.164
2	312.638	1.152
3	317.652	1.171
4	322.464	1.156
5	331.375	1.159
6	360.253	1.140

Instrument (OMI) on the NASA EOS Aura satellite, especially in the Southern Hemisphere.

For radiance, the highest radiances observed by channels 3 and 4 are close to the maximum values from simulations using the MODTRAN RTM. For channels 5 and 6, the observed radiances of TOU exceed the simulated maximum values. It was also found that these two channels become saturated for the brightest scenes at low solar zenith

angles—that is, at the highest signal levels. For the lower range of radiance, the TOU has a better agreement with OMI in total column ozone but has much larger differences when the radiances for channel 6 are greater than 6.6 $\mu\text{W}/\text{cm}^2/\text{sr}/\text{nm}$. After examining the pre-launch calibration, it was found that the TOU response function for each channel was only measured in the lower range of radiances with a gain range ratio determined by the output voltage of

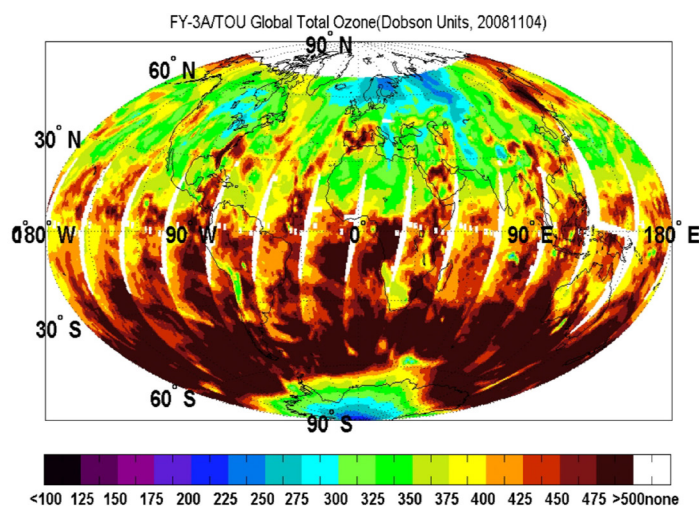


Figure 1a. Total column ozone for November 4, 2008, as retrieved from the TOU before cross-calibration.

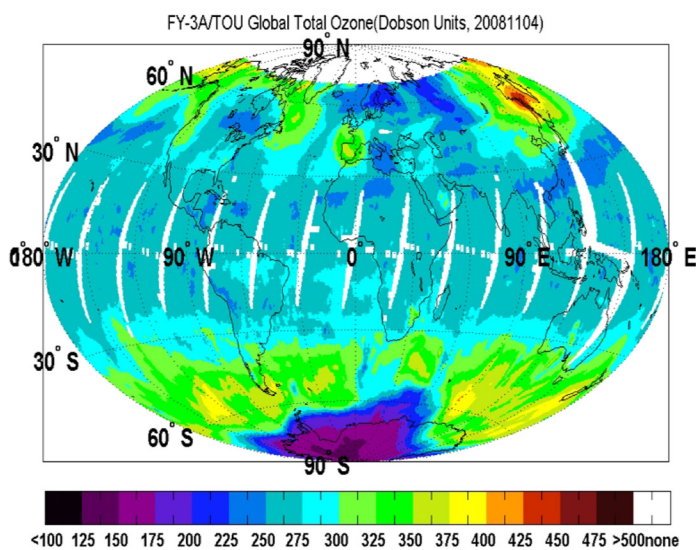


Figure 1b. Total column ozone retrieved from the TOU after cross-calibration.

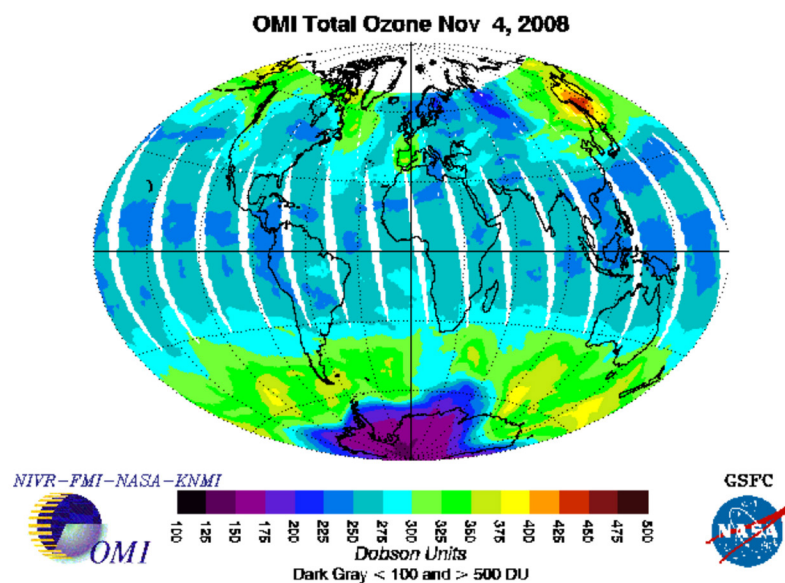


Figure 1c. Total column ozone retrieved from OMI.

each channel. The gain range ratio was also measured over the same range of radiances, and the linearity was derived from all radiance ranges. Although the TOU detector is highly linear in all radiance ranges, it is possible that it has a different response function for different radiance ranges. Unfortunately, the response function was not measured for all ranges of radiance in the pre-launch calibration and the limited characterizations were applied to all measurements in the on-orbit calibration processing.

The Level 3 ozone and effective reflectivity products from OMI are used as input to a radiative transfer model to predict the TOU radiances and characterize the biases for the measurements over the Pacific Ocean in low and mid latitudes. Coefficients are derived from a regression algorithm to adjust the TOU radiances. It was found that after the measurement bias corrections, the biases between the retrieved total column ozone products from the TOU with those from the OMI TOMS-V8 products and those from a set of ground-based station measurements are reduced to 3 percent and 5 percent, respectively. The variations in the estimated total ozone amounts from the TOU are consistent with those derived from Solar Backscatter Ultraviolet (SBUV/2) instruments and OMI for a period from January 2010 to February 2011. Figures 1a, 1b, and 1c show an example of before-and-after maps from the TOU compared with a map for the same day from OMI.

[Rate and comment on this article](#)

Measurement of Atmospheric Composition using UV-visible Spectrometers from Geostationary Orbits

by Jhoon Kim, Department of Atmospheric Sciences, Yonsei University, Seoul, Korea

Regular monitoring of the ozone layer from space began with the Solar Back-scattered Ultraviolet (SBUV) and the Total Ozone Monitoring Spectrometer (TOMS) on Nimbus-7 in late 1978. These measurements have continued since 2004 to date with Ozone Monitoring Instrument (OMI) on EOS Aura. With the recent development of spectrometers in UV-visible with sub-nm spectral resolution and development of retrieval algorithms, we now can generate estimates of the column amounts of atmospheric O₃, NO₂, SO₂, HCHO, CHOCHO and other constituents in the troposphere and stratosphere. To date, all the UV-visible satellite missions to monitor trace gas concentrations in the atmosphere have been in low Earth orbits (LEOs), usually allowing one observation per day. With the advent of new UV-visible instruments on geostationary (GEO) platforms, the diurnal variation of these components now can be captured.

The GEMS (Geostationary Environment Monitoring Spectrometer) is to be launched into orbit at the end of 2018. It will be positioned over Asia. The instrument is basically a step-and-stare scanning UV-visible imaging spectrometer, with scanning Schmidt telescope and Offner spectrometer. A UV-enhanced 2D CCD takes images, with one axis spectral and the other north-south spatial, with east-west scanning over time. On-orbit calibrations are planned, making daily solar measurements and weekly LED light source linearity checks. For the solar calibration, there are two transmissive diffusers, a daily working one and a reference diffuser used twice a year to check the degradation of the working one. Dark current measurements are planned twice a day, before and after the daytime imaging. In order to avoid dark current issues and random telegraph signal (RTS), the CCD is

cooled to temperatures well below 0° C.

Spectral stability is required to be better than 0.02 nm over 24 hours, stray light less than 2 percent, polarization sensitivity less than 2 percent at the instrument level, and the instrument system level MTF better than 0.3. Preflight calibration will be carried out by using the NIST standards.

By 2020, the geostationary orbits are expected to be filled with three UV-visible spectrometers:

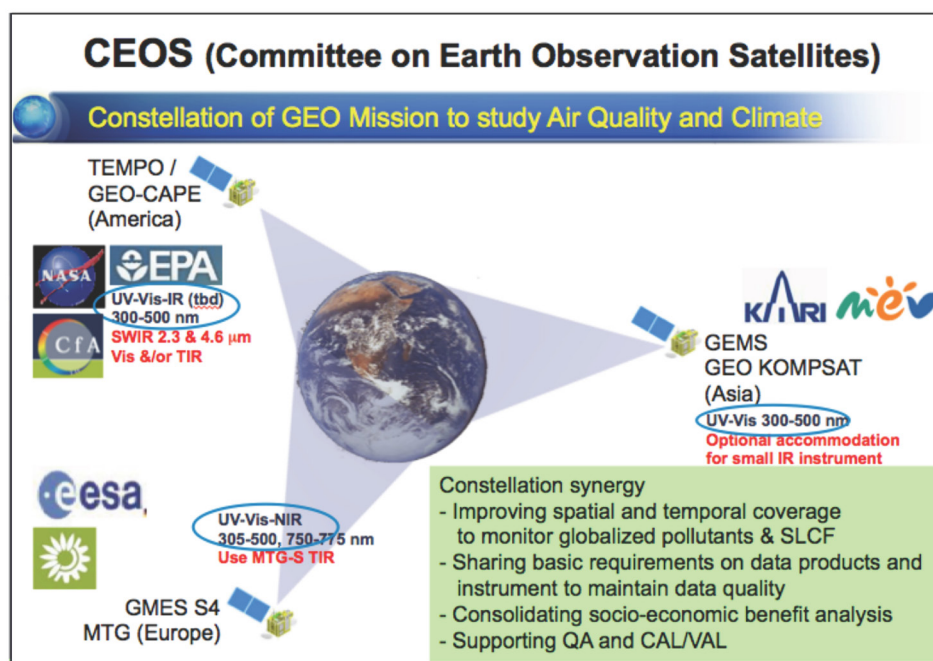
- The NASA Tropospheric Emissions: Monitoring of Pollution (TEMPO) (P.I.: Kelly Chance, Harvard-Smithsonian Center for Astrophysics) over North America
- The ESA Sentinel-4 Ultraviolet Visible Near infrared (UVN) spectrometer over Europe (Mission Scientist: Ben Veihelmann, ESTEC)
- The KARI GEMS over Asia (P.I.: Jhoon Kim, Yonsei University), with the Tropospheric Monitoring

Instrument (TROPOMI, P.I.: Pepijn Veefkind, KNMI) flying underneath in LEO.

Recognized by the Committee on Earth Observing Satellite (CEOS) Atmospheric Composition Constellation (ACC), the geostationary constellation of UV-visible spectrometers will enlighten us on the global distribution of ozone, aerosol, and their precursors. To integrate the dataset for global measurements, harmonized data quality is very important. Thus the inter-calibration among the three different UV-visible satellite instruments is very important, in addition to the quality of the data processing. Therefore, the standardization of data products and pre-calibration/post-calibration/validation methods are being discussed. Participation in the GSICS UV subgroup would surely make a great contribution to future activities of geostationary constellation programs.

	GEMS	TEMPO	Sentinel-4
Spectral ranges (nm)	300–500	290–490 / 540–740	305–500 / 750–775
Spectral resolution (nm)	0.6 (3 samples)	0.6 (3 samples)	0.5 / 0.12
Spatial Resolution (NS km × EW km)	7 × 8 @ Seoul 3.5 × 8 for aerosol	2.1 × 4.7	8 × 8 @ 45° N
Spatial coverage	5°S–45°N 75°E–145°E	19°N–57.5°N 73°W–130°W	30°N–65°N 30°W–150°W
Obs. time	30 min	1 hour	1 hour
Onboard calibration	Solar, cal light source	Solar	Solar, cal light source
Volume (m3)	1.1 × 1.2 × 0.9	1.0 × 1.1 × 1.0	1.1 × 1.2 × 0.9
Mass (Kg)	140	100	150
Power (W)	200 (on orbit) / 100 (transfer)	100	180
Data rate (Mbps)	40	30	25

Source: Kelly Chance, Ben Veihelmann



References

Committee on Earth Observation Satellites Atmospheric Composition Constellation (CEOS ACC), 2011, *A Geostationary Satellite Constellation for Observing Global Air Quality: An International Path Forward*, position paper.

Chance, K., 2014, Overview of TEMPO status. *TEMPO Science Team Meeting*, Hampton, VA.

Kim, J., 2014, Overview and status of GEMS. *TEMPO Science Team Meeting*, Hampton, VA.

Veihelmann, B., 2013, Sentinel-4 status. *CEOS ACC-9 meeting*, Darmstadt, Germany.

[Rate and comment on this article](#)

The MAESTRO Spectrophotometer on the Atmospheric Chemistry Experiment

by C.T. McElroy, York University, Canada

The Atmospheric Chemistry Experiment (ACE) on the Canadian Space Agency's (CSA) SCISAT satellite was launched on an Orbital Sciences Pegasus launcher August 12, 2003, from Vandenberg Air Force Base. The mission was primarily designed to take measurements of the Arctic stratosphere to monitor ozone chemistry and particularly the evolution of the ozone layer in the late winter and early spring. The satellite includes two instruments, an infrared Fourier Transform Spectrometer (FTS) built by ABB, Inc., of Quebec City and the Measurements of Aerosol Extinction in the Stratosphere and Troposphere Retrieved by Occultation (MAESTRO) Spectrophotometer constructed by a group that included members from Environment Canada (EC), University of Toronto, and EMS Technologies, Inc. (now COM-DEV, Inc.). The FTS measures 40+ chemical species while MAESTRO is intended to provide wavelength-dependent aerosol extinction measurement.

The Instrument

MAESTRO (McElroy et al., 2007) is a dual, concave holographic grating spectrometer. Each half has a 1024-element RETICON detector. The ACE-

FTS has an internal tracking mirror that centers the FTS field-of-view on the sun and a pick-off mirror that relays part of the beam to MAESTRO. A beam-splitter provides light to the UV and visible halves of MAESTRO (see Table 1).

Table 1. Main characteristics of the ACEMAESTRO instrument spectrometers.

Characteristic	UV Spectrophotometer	Visible Spectrophotometer
Nominal Wavelength Range	285–550 nm	525–1,020 nm
Calibrated Wavelength Range in Occultation	400–545 nm (pixels 463 - 954)	520–1010 nm (pixels 21 - 1010)
Spectral Resolution	~1.5 nm	~2 nm
Main Absorbers	O ₃ , NO ₂ , aerosols	O ₂ , O ₂ -O ₂ , H ₂ O, aerosols
Secondary Absorbers	SO ₂ , OClO, BrO, HCHO, CH ₃ CHO	NO ₂
General		Characteristic
SCISAT Orbit		Circular, 650 km, 74° Inclination
Vertical Resolution		~1.2 km (bestcase resolution, at 22 km tangent)
Observation Modes		Solar Occultation and Nadir Backscatter
Detectors		1024pixel, Reticon photodiode array
Diffraction Gratings		Concave holographic, 94 mm focal length
Signal to Noise Ratio		~1000–3000 (at High Sun)
Mass		8 kg
Power		14 W

For an orbit which goes directly toward or directly away from the Sun (beta angle = 0°), the tangent ray from the sun changes altitude by approximately 3 km per second. Spectra must be collected at $\sim 3 \text{ s}^{-1}$ to match the MAESTRO vertical resolution of $\sim 1 \text{ km}$.

To meet speed and signal-to-noise requirements, a sophisticated detector readout scheme uses a soft-programmable, Xilinx Field-Programmable Gate Array (FPGA). An 8-bit microprocessor core in the FPGA and a custom-designed state machine, coupled to the processor as a peripheral, is used to sequence reading of the RETICON. Different modes of reading and co-adding are used to optimize the signal-to-noise ratio of each spectrum. The goal is to fill each of the detector wells as full as possible in the $\sim 300 \text{ ms}$ available to make a measurement.

Data Collection and Analysis

Solar occultation data have a very large dynamic range—of the order of 3000:1. There is also a large gradient in intensity with wavelength, particularly in the UV $\sim 10^4$:1 or more. To accommodate, the system has different modes including co-adding, reading the detector in pixel groups, and reading individual pixels between photodiode resets.

The data are analyzed in steps. Dark count, High Sun reference, and occultation spectra are converted to counts. Occultation and High Sun spectra are corrected for dark count and offset. The average of 20 High Sun spectra is used as a reference and compared to a High resolution extraterrestrial spectrum to calibrate its wavelength scale. Optical depth spectra created by ratioing the occultation data to the reference spectrum are fitted with a spectral fitting code to determine the column densities of ozone, water, oxygen, NO_2 , and $\text{O}_2\text{-O}_2$. Offset, linear, quadratic, and cubic vectors are included as a proxy for aerosol absorption. Shift and stretch of the wavelength scale is also done simultaneously. Tangent altitudes are determined by comparing the MAESTRO and FTS ozone. The FTS determines heights from the P-T profile retrieved using CO_2 absorption.

Using retrieved gas amounts and air columns from the FTS atmosphere, the optical depth spectra are fitted and the residual attenuation summed with the polynomial vector contributions to produce the aerosol wavelength-depen-

dent extinction. Figure 1 shows ozone profiles from MAESTRO and FTS on February 23, 2004. Figure 2 shows an aerosol profile.

MAESTRO data are in the ACE archive at University of Waterloo during

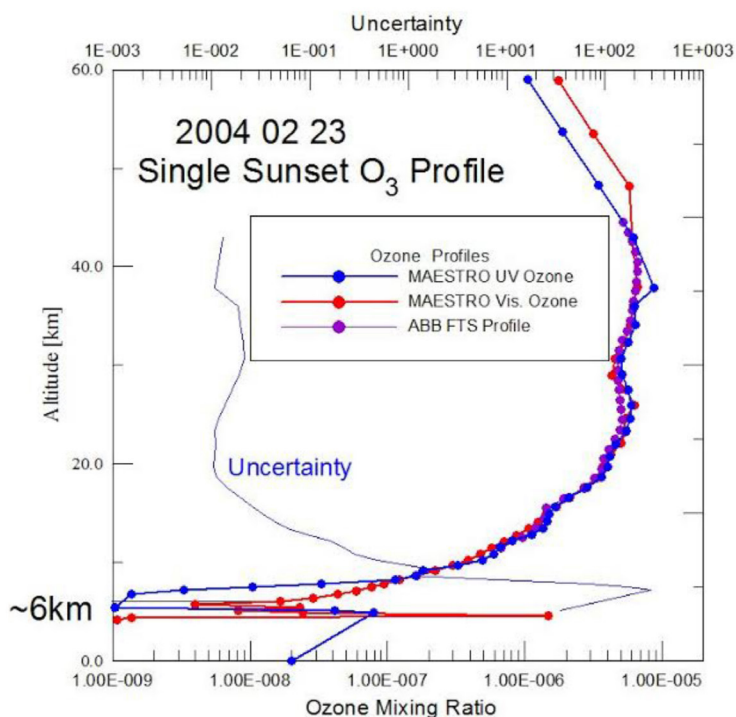


Figure 1: Ozone profiles retrieved by the UV and visible halves of MAESTRO in the Chappuis band compared to an FTS profiles taken at the same time.

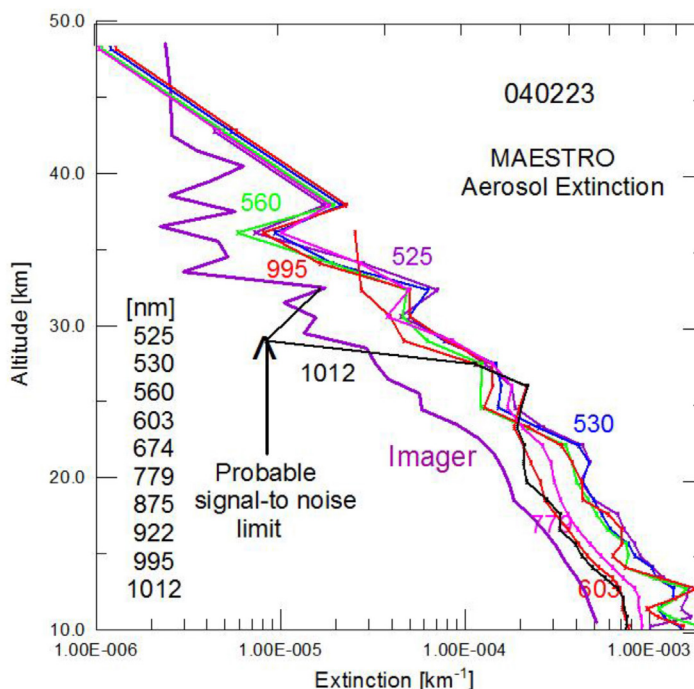


Figure 2: Aerosol vertical profiles at a number of wavelengths compared to an FTS Imager profile at $1 \mu\text{m}$. Vertical profiles of the Ångström coefficient are also produced.

the period February 2004 to the present (<http://www.ace.uwaterloo.ca/>). Researchers wanting MAESTRO data should contact Kaley Walker (kwalker@atmosp.physics.utoronto.ca). Information about processed data is available from Jason Zou (jzou@atmosp.physics.utoronto.ca) and instrument-related information from the author (tmcelroy@yorku.ca).

Acknowledgements

MAESTRO was created with support from CSA and the European Community (EC). Jason Zou and Florian Nichitiu are responsible for MAESTRO operations. James Drummond is a co-investigator. Peter Bernath is ACE mission scientist. and Kaley Walker, deputy mission scientist.

Reference

McElroy, C.T., Nowlan, C.R., Drummond, J.R., Bernath, P.F., Barton, D.V., Dufour, D.G., Midwinter, C., Hall, R.B., Ogyu, A., Ullberg, A., Wardle, D.I., Kar, J., Zou, J., Nichitiu, F., Boone, C.D., Walker, K.A., and Rowlands, N., 2007, The ACE-MAESTRO instrument on SCISAT: description, performance, and preliminary results. *Applied Optics*, 46, 20, 4341–4356.

[Rate and comment on this article](#)

News in this Quarter

The NASA Orbiting Carbon Observatory-2 is on its Way!

by David Crisp, NASA

The Orbiting Carbon Observatory-2 (OCO-2) is NASA's first dedicated CO₂ monitoring satellite. It was successfully launched from Vandenberg Air Force Base on a Delta-II 7320 launch vehicle at 2:56 a.m. PDT on July 2, 2014. The launch vehicle targeted an initial orbit about 15 km below the 705-km Afternoon Constellation (A-Train). The A-Train currently includes six other Earth observing satellites that fly in formation in a near-polar, Sun-synchronous orbit that crosses the Equator near 1:30 p.m. Preliminary spacecraft checkout activities were completed during the first week of operations. Over the next four weeks, OCO-2 used its onboard propulsion system to execute a series of orbit-raising maneuvers to take up its position at the head of the A-Train constellation. Once in the A-Train, the instrument optical bench and detectors were cooled to their operating temperatures and a week-long observatory checkout period commenced. OCO-2 started routinely collecting and returning science data in late August.

Fossil fuel combustion, deforestation, and other human activities are currently adding almost 40 billion tons of carbon

dioxide (CO₂) to the atmosphere each year. These CO₂ emissions are superimposed on active natural carbon cycle that emits more than 20 times as much CO₂ into the atmosphere each year as human activities, and then reabsorbs a comparable amount, along with about half of the human contributions. Existing ground-based measurements provide a strong global constraint on both human and natural CO₂ fluxes into the atmosphere. However, much greater resolution and coverage are needed to identify and characterize the strongest natural sources and sinks, and to discriminate the human CO₂ emissions from the natural background. Such measurements are essential to any carbon management.

One way to improve the spatial and temporal sampling of CO₂ is to retrieve precise, spatially resolved, global estimates of the column-averaged CO₂ dry air mole fraction (X_{CO₂}) from space. Surface weighted X_{CO₂} estimates can be retrieved from high resolution spectroscopic observations of reflected sunlight in near infrared CO₂ and O₂ bands. This is a challenging space-based remote sensing observation because even the largest CO₂ sources and sinks produce

changes in the background X_{CO₂} distribution no larger than 2 percent, and most are smaller than 0.25 percent. The European Space Agency (ESA) Envisat SCIAMACHY and Japanese Greenhouse Gases Observing Satellite (GOSAT) TANSO-FTS were the first satellite instruments designed to exploit this measurement approach. SCIAMACHY collected column-averaged CO₂ and methane (X_{CH₄}) measurements over the sunlit hemisphere from 2002 to 2012. TANSO-FTS has been collecting X_{CO₂} and X_{CH₄} observations since April 2009. These data have provided an excellent proof of concept and are beginning to yield new insights into the carbon cycle, but improvements in sensitivity, resolution, and coverage are still needed.

OCO-2 is a "carbon copy" of the Orbiting Carbon Observatory, which was lost in 2009 when its launch vehicle malfunctioned and failed to reach orbit. OCO-2 carries and points a three-channel, imaging, grating spectrometer. This instrument collects high resolution spectra of reflected sunlight in the 765 nm O₂ A-band and in the 1,610 and 2,060 nm CO₂ bands with unprecedented sensitivity. Each channel collects 24 spectra per

second, yielding about a million samples each day over the sunlit hemisphere. Coincident measurements from the three channels are combined and analysed with a “full-physics” retrieval algorithm to yield estimates of X_{CO_2} . Clouds and optically thick aerosols preclude observations of the full atmospheric column in many regions, but this approach is expected to yield over 100,000 full-column X_{CO_2} estimates each day.

The OCO-2 Measurement Strategy

For routine science operations, the instrument’s bore sight is pointed to the local nadir or at the *glint spot*, where sunlight is specularly reflected from the Earth’s surface. Nadir observations provide the best spatial resolution and are expected to yield more cloud-free X_{CO_2} soundings. Glint observations will have much better signal-to-noise ratios (SNR) over dark ocean surfaces. The nominal plan is to alternate between glint and nadir observations on consecutive 16-day ground-track repeat cycles, so that the entire sunlit hemisphere is sampled in both modes at 32-day intervals. OCO-2 can also target selected surface calibration and validation sites and collect thousands of observations as the spacecraft flies overhead. The instrument’s rapid sampling, small ($< 3 \text{ km}^2$) sounding footprint, and high sensitivity, combined with the spacecraft’s ability to point the instrument’s bore sight toward the glint spot over the entire sunlit hemisphere, are expected to provide improved coverage of the ocean, partially cloudy regions, and high latitude continents than earlier missions.

The OCO-2 team expects to start delivering calibrated, geo-located spectral radiances to the NASA Goddard Earth Sciences Data and Information Services Center (GES DISC) by late December of this year. The first X_{CO_2} products will begin within 90 days of that.

GRUAN-GSICS-GNSSRO WIGOS Workshop on Upper-Air Observing System Integration and Application

by Tim Hewison, Xavier Calbet, and Axel von Engel, EUMETSAT

On 6–8 May 2014 a workshop was convened at WMO in Geneva to investigate ways in which ground-based observations, satellite sounders, and radio occultation could contribute to the WMO Integrated Global Observing System (WIGOS). Representatives of these communities, together with Numerical Weather Prediction (NWP) and GSICS, spent three intensive days discussing ideas to enhance their future interactions. After hearing the attendees’ position statements, the workshop went on to debate four main themes:

1. Applications and Required Dataset Generation—facilitated by Greg Bodeker
2. Measurement Uncertainty Estimation and Terminology—facilitated by Holger Vömel
3. Observing System Coordination and Collocation—facilitated by Xavier Calbet
4. Participation and Outreach—facilitated by Stephan Bojinski

At the workshop it was recognized that it would be extremely beneficial to compare atmospheric profiles from different observing systems (GRUAN radiosondes and satellite sounder and radio occultation profiles). This comparison would highlight any potential inconsistencies among the datasets which could arise from any remaining systematic uncertainties present in the data. It would also provide an *inter-calibration bridge* between different observing systems. In order for these inter-comparisons to be effective, it is essential to gain a full understanding of the uncertainties associated with each system. This knowledge is also necessary to allow the observing systems to be combined in an optimal way within

the NWP data assimilation system. The uncertainties in comparisons between different observations are often dominated by variability in the atmosphere (clouds, humidity, etc.) or the surface (reflectivity, temperature, etc.)—both in space and time.

A joint [white paper](#) has recently been produced describing the current situation in defining potential collocation criteria for GRUAN and satellite measurements. To follow this up, it was agreed to perform a comparison of different methods to estimate the uncertainties in the collocation of different observing systems for a common time period, based on observations of various satellite instruments collocated with GRUAN upper air stations.

Of the many other topics discussed, another one of interest to GSICS was the idea of comparing profiles retrieved from radio occultation systems with radiances observed by the sounding channels of microwave sounders (in radiance space, using radiative transfer models). In this context, the GNSSRO profiles could provide a reference against which to validate the inter-calibration of these microwave instruments.

It was also agreed that there should be cross-representation of the different communities. For example, GSICS members have been asked to attend meetings of the AOPC Working Group on GRUAN. This will further help us work together toward the goals of the WMO Integrated Global Observing System.

The full report of the meeting will be published on the [WMO website](#).

Summary of GSICS Executive Panel Meeting

by Jerome Lafeuille, WMO

The 15th meeting of GSICS Executive Panel was held in Guangzhou, China, on 16 and 17 May 2014. The meeting was attended by representatives of CMA, CNES, EUMETSAT, JAXA, JMA, KMA, NASA, NOAA, ROSHYDROMET, WMO, and GSICS/GDWG, with

remote participation of ISRO, USGS, Mitch Goldberg, and the chairpersons of GCC, GRWG, and CEOS/WGCV. CNSA also attended as an observer.

The meeting marked an important milestone in GSICS governance: Dr. Mitch Goldberg stepped down as the Chair of the GSICS Executive Panel. Dr. Goldberg chaired the Executive Panel since the creation of GSICS. The Panel members thanked Mitch for his enthusiastic leadership over 8 years, while expecting that he will continue to bring his expertise as the NOAA delegate. Peng Zhang, CMA, was elected as the new Chair and Ken Holmlund, EUMETSAT, Vice-Chair. The Panel congratulated Mitch, Peng, and Ken and was pleased to note that this rotation of responsibility illustrated the international dimension of GSICS and encourages all members to be fully engaged in GSICS. The Panel designated Masaya Takahashi as Vice-Chair of GRWG, and approved the terms of reference for the EP Chair and GRWG Chair.

The Panel recalled the *Vision of GSICS in the 2020s* depicting GSICS as a “collaborative framework among satellite operators and science teams to develop, implement and share best practices, procedures and tools to monitor, improve and harmonize the calibration of environmental satellites of the global observing system.” It stressed that the focus should remain the systematic generation of in-orbit inter-calibration information to refine the calibration of Level 1 satellite data, in accordance with GSICS core principles, in support of CGMS satellite operators, satellite users, and WMO programs.

The Panel welcomed the reports from GCC, GDWG, GRWG, and all the agencies on the progress of their respective activities, and commended the GCC and all contributors for the *GSICS Quarterly*. The Panel recalled the important role of the GCC to support the implementation of the Procedure for Products Acceptance, to maintain the GSICS Product Catalogue and coordinate efforts of GPRCs to bring products to the pre-operational and ultimately to the operational stage, under approval by

the Panel. The Panel urged the GCC and GPRCs to submit candidate GEO-LEO Infrared products for endorsement as operational products. It welcomed the progress made within GRWG on solar channel and on microwave calibration. It underscored the value of the Moon as a transfer standard for visible and SWIR calibration and strongly supported the proposal from EUMETSAT to hold a lunar calibration workshop.

The Panel highlighted the role of GSICS in the Architecture for Climate Monitoring from Space. In this regard GSICS should provide methods, best practices or standards for inter-calibration, ensure the availability of in-orbit reference standards to provide traceability, and ensure the availability of reference data sets with documented uncertainty, or contribute to composite reference data sets (e.g., with GCOS/GRUAN). It was recalled that, as stated in the GSICS Vision, the production of Fundamental Climate Data Records (FCDR) was not within the scope of GSICS. Therefore, in spite of its scientific value, the Panel clarified that the MSU/AMSU FCDR generation could benefit from GSICS but was not a GSICS product and should be removed from the GSICS catalog. Instead, it encouraged the GCC and relevant GPRCs to submit a microwave inter-calibration correction product for its approval when such product will be available. The Panel invited the GCC to increase its communication efforts to better inform the users on the definition of GSICS products, what products are available, how to access them, and how they can be used. Upon a suggestion to relax the GPPA for third-party products, and following a lively discussion, the Panel reaffirmed that the GPPA should guarantee rigor, maturity, and reliability of a product development process, for GSICS or other products.

Finally, the Panel welcomed the offer from CMA to host the next user workshop in the context of the Fifth Asia-Oceania Meteorological Satellite Users Conference in Shanghai in October 2014.

A Note from the Executive Panel Chair

by Peng Zhang, CMA



This is my first message to the GSICS community as Chair of its Executive Panel, and I am pleased to recall my first interaction with the community way back in January 2007 and my

first time using telecommunications as a mode to give a presentation. The first GRWG workshop was held at NOAA that year, and I can clearly remember the presentation I made—via telecom in the middle of the night during a Beijing winter!

For the first time, I introduced the inter-calibration activities of CMA to GSICS. I feel very lucky that I could be involved in GSICS from its very beginning. The GSICS community strengthened my understanding of the goal of satellite calibration and the role of GSICS.

As time progressed, CMA was able to use GSICS methodologies to improve Fengyun satellite calibration in many aspects. Notably, the inner blackbody calibration problem was solved and the radiance calibration uncertainty was reduced from the original 4K degree to the current 1K degree for the FY-2 series. The O-B method has been used to monitor the data quality of the infrared sounder and the microwave sounder of the FY-3 satellites. The multi-sites, DCC, and the lunar method have been used to monitor the data quality of the reflection bands of the FY-2 and FY-3 satellites. All this progress represents benefits derived from the GSICS community.

I wish to express sincere thanks to Dr. Mitch Goldberg, one of the founders of GSICS. His enthusiastic leadership enabled GSICS to become a truly international community. Over the past eight years, the GSICS role in reducing satellite calibration anomalies has grown, and each participating agency has benefited.

Dr. Goldberg leaves Kenneth Holmlund and me a very well-defined and well-developed GSICS. I doubt if I have the capability to lead GSICS as productively and successfully as Dr. Goldberg has done. What I can only do is to try my best to serve GSICS.

We have a common mission and vision among GSICS members that will continue to guide us well into the future. We believe GSICS is on the right path to construct the collaborative framework among satellite operators and science teams to develop, implement, and share best practices, procedures, and tools to monitor, improve, and harmonize the calibration of environmental satellites of the global observing system.

Announcements

GSICS Users Workshop to be Held 19-21 Nov, 2014 in Shanghai

by Manik Bali, NOAA

The 2014 GSICS Users workshop is to be held from 19–21 November 2014 in Shanghai, China. This workshop will be a part of the Fifth Asia-Oceania Meteorological Satellite Users Conference.

The GSICS Users workshop will cover topics including but not limited to calibration and correction of measured radiances in MW, IR, and VIS. Studies on impact of using GSICS-corrected radiances on generating products downstream like Level 2 would be particularly interesting during the workshop. In addition, the Users Workshop will focus on discussing topics that would encourage international collaboration among GSICS members.

Please contact Ms. Xu Hanlie, xuhanlie@cma.gov.cn, to submit an abstract, or follow the [link](#) to get more information. The abstract may also be sent to the GSICS Coordination Center (manik.bali@noaa.gov).

GSICS Lunar Calibration Workshop to be Held in Darmstadt, Germany

by Sebastien Wagner, EUMETSAT, T. Stone, USGS, S. Lachérade, CNES, B. Fournie, CNES and X. Xiong, NASA

In recent years, space and meteorological agencies operating Earth observing satellites have shown an increasing interest in lunar calibration for monitoring the temporal stability of their instruments. Both GSICS and CEOS IVOS recommend lunar calibration as a calibration and inter-calibration method for VIS/NIR bands that should be implemented for instruments that have the capability to sense the Moon. The current reference model for lunar calibration (the so-called ROLO model) has been developed and is being maintained by the United States Geological Survey (USGS). A few agencies have implemented their own version of this model. However, experience has shown that there could be differences between some of these independent implementations and the official USGS version of the ROLO model.

During the last GSICS Research and Data Working Group annual meeting in Darmstadt (24–28 March 2014), the GSICS community, together with the CEOS-IVOS chairman (Nigel Fox, from NPL) recommended harmonizing the

version of the ROLO model used for lunar calibration of VIS/NIR satellite instruments by more and more operators. Indeed, in the context of instrument inter-calibration, use of the same transfer reference should be ensured.

EUMETSAT offered to host a lunar calibration workshop to initiate an activity to share knowledge on lunar calibration and to promote the use of a common reference across participating groups. This workshop is being organized by EUMETSAT, USGS, CNES, and NASA.

The main objectives of the workshop are:

- To work across agencies/operators with a common and validated implementation of the USGS ROLO model. For that, a reference GSICS implementation of the model has to be considered.
- To make a reference model, based on the EUMETSAT ROLO implementation, available to groups working with lunar observations from Earth observing satellites.
- To share knowledge and expertise on lunar calibration.
- To generate for the first time a reference dataset that could be used for validation/comparisons and development of GSICS inter-calibration products later on.

This workshop would be the first step in providing the international commu-

nity with a referenced and traceable version of the USGS ROLO model. Such a model, called GSICS Implementation of the ROLO model (GIRO), would be usable to transfer the calibration between different instruments and to generate inter-calibration products—even from different eras—supporting the generation of Fundamental Climate Data Records.

One of the key benefits of the workshop would be to generate for the first time a reference dataset comparing observations from a range of satellite instruments using a common lunar irradiance model. This would be used to identify shortcomings in the existing model and develop and validate future improvements.

A kickoff web meeting was organized on June 24 where many groups (35 attendees!) showed interest in attending the workshop. Participants are asked to prepare their data and to process them with GIRO, which is expected to be made available in September. The workshop is foreseen to be held in December 2014 or January 2015. More information and documentation regarding the preparation of the data and the workshop, together with the contact details of the organizers, can be found in the GSICS Development Wiki topic: <https://gsics.nesdis.noaa.gov/wiki/Development/20140624>.

GSICS-Related Publications

- Cao, C., De Luccia, F., Xiong, X., Wolfe, R., and Weng, F., 2014, Early on-orbit performance of the visible infrared imaging radiometer suite onboard the Suomi National Polar-Orbiting Partnership (S-NPP) Satellite. *IEEE Transactions on Geoscience and Remote Sensing*, 52, 1142–1156.
- Chen, L., Hu, X., Xu, N., and Zhang, P., 2013, The application of deep convective clouds in the calibration and response monitoring of the reflective solar bands of FY-3A/MERSI (Medium Resolution Spectral Imager). *Remote Sens.*, 5, 6958–6975.
- Emery, W.J., Good, W.S., Tandy, W. Jr., Izaguirre, M.A., and Minnett, P.J. A microbolometer airborne calibrated infrared radiometer: The Ball Experimental Sea Surface Temperature (BESST) Radiometer. *IEEE Transactions on Geoscience and Remote Sensing*, 52, 7775–7781.
- Fan, X., and Liu, X., 2014, Quantifying the relationship between intersensor images in solar reflective bands: Implications for intercalibration. *IEEE Transactions on Geoscience and Remote Sensing*, 52, 7727–7737.
- Gierens, K., Eleftheratos, K., and Shi, L., 2014, Technical Note: 30 years of HIRS data of upper tropospheric humidity. *Atmos. Chem. Phys.*, 14, 7533–7541.
- He, W., Zou, C., and Chen, H., 2014, Validation of AMSU-A measurements from two different calibrations in the lower stratosphere using COSMIC radio occultation data. *Chinese Science Bulletin*, 59, 1159–1166.
- Kim, B., Ham, S.-H., Kim, D., and Sohn, B.-J., 2014, Post-flight radiometric calibration of the Korean geostationary satellite COMS meteorological imager. *Asia-Pacific Journal of Atmospheric Sciences*, 50, 201–210.
- Kim, D.H., and Ahn, M. H., 2014, Introduction of the in-orbit test and its performance for the first meteorological imager of the Communication, Ocean, and Meteorological Satellite, *Atmos. Meas. Tech.*, 7, 2471–2485, doi:10.5194/amt-7-2471-2014.
- Mesiter, G., and Franz, B., 2014, Corrections to the MODIS Aqua calibration derived from MODIS Aqua ocean color products. *IEEE Transactions on Geoscience and Remote Sensing*, 52, 6534–6541.
- Roithmayr, C.M., Lukashin, C., Speth, P.W., Kopp, G., Thome, K., Wielicki, B.A., and Young, D.F., 2014, CLARREO approach for reference intercalibration of reflected solar sensors: On-orbit data matching and sampling. *IEEE Transactions on Geoscience and Remote Sensing*, 52, 6762–6774.
- Roithmayr, C.M., Lukashin, C., Speth, P.W., Young, D.F., Wielicki, B.A., Thome, K.J., and Kopp, G., 2014, Opportunities to intercalibrate radiometric sensors from International Space Station. *J. Atmos. Oceanic Technol.*, 31, 890–902. doi: <http://dx.doi.org/10.1175/JTECH-D-13-00163.1>.
- Stone, T., 2014, Back-calibration and cross-calibration of Earth observing imagers using the Moon as a common radiometric reference. *NEWRAD 2014 Conference in Espoo, Finland*. http://newrad2014.aalto.fi/Newrad2014_Proceedings.pdf.
- Xu, N., Chen, L., Hu, X., Zhang, L., and Zhang, P., 2014, Assessment and correction of on-orbit radiometric calibration for FY-3 VIRR thermal infrared channels. *Remote Sens.*, 6, 2884–2897.
- Wu, X., Liu, Q., Zeng, J., Grotenhuis, M., Qian, H., Caponi, M., Flynn, L., Jaross, G., Sen, B., Buss, R.H. Jr., Johnsen, W., Janz, S., Pan, C., Niu, J., Beck, T., Beach, E., Yu, W., Rama Varma Raja, M.K., Stuhmer, D., Cumpston, D., Owen, C., and Li, W.-H., 2014, Evaluation of the sensor data record from the nadir instruments of the Ozone Mapping Profiler Suite (OMPS). *J. Geophys. Res. Atmos.*, 119, 6170–6180, doi:10.1002/20.
- Zhong, B., Zhang, Y., Du, T., Yang, A., Lv, W., and Liu, Q., 2014, Cross-calibration of HJ-1/CCD over a desert site using Landsat ETM+ imagery and ASTER GDEM product. *IEEE Transactions on Geoscience and Remote Sensing*, 52, 7247–7263.

Submitting Articles to GSICS Quarterly Newsletter:

The next issue of the GSICS Quarterly would be a special issue on Visible Channel. Dave Doelling from NASA would lead it. For this issue we are looking for short articles (~ 700 words with one or two key, simple illustrations), especially related to cal/val capabilities and how they have been used to positively impact weather and climate products. Unsolicited articles are accepted anytime, and will be published in the next available newsletter issue after approval/editing. Please send articles to Manik Bali (manik.bali@noaa.gov).

With Help from our Friends:

The GSICS Quarterly Editor would like to thank those individuals who contributed articles and information to this newsletter. The Editor would also like to thank our European Correspondent, Dr. Tim Hewison of EUMETSAT, American Correspondent, Dr. Fangfang Yu of NOAA, Asian Correspondent, Dr. Yuan Li of CMA, and Larry Flynn, GCC Director, in helping to secure and edit articles for publication.

The Editor would also like to thank Dr. Lawrence E. Flynn for reviewing the articles in the Newsletter and Dr. Chunhui Pan for proof reading the Newsletter

GCC team welcomes your [feedback](#) and suggestions about the GSICS Quarterly.